A Two-parameter Representation of the Normal Temperature Distribution of the 1,000—500 mb Layer

By G. ÁRNASON[1] and L. VUORELA[2], University of Stockholm

(Manuscript received June 14, 1954)

Abstract

Height normals for 1,000, 700 and 500 mb, published by U.S. Weather Bureau, have been used to study the normal temperature field of the 1,000—500 mb layer by means of a simple model. In this model the normal temperature-height curve is replaced by one having a temperature lapse-rate independent of height in such a way that the thicknesses of the sub-layers 1,000—700 and 700—500 mb are correctly represented by the model. As a consequence, the temperature as well as its horizontal gradient and the thermal wind all have a linear variation with height and may be described in terms of two parameters, the temperature lapse-rate k and a "representative" 1,000 mb temperature τ_0.

Hemispheric maps for these parameters as well as the thermal wind at 1,000 and 500 mb have been prepared for the months January and July. The major frontal zones of the atmosphere appear clearly on the τ_0-maps in positions which agree essentially with those shown earlier by a number of meteorologists. The July map reveals, however, a strong baroclinic zone in high latitudes, surrounding the polar cap, not shown clearly in earlier presentations of the low-level baroclinity.

The k-charts disclose large horizontal variation in the temperature lapse-rate, and the charts for the thermal wind show that its variation with height is very pronounced in middle and high latitudes.

1. Introduction

Until recently, reliable hemispheric charts displaying the normal distribution of various meteorological elements have not been available, except for surface data and those meteorological phenomena which could be observed from the ground. The greatly improved network of upper air stations since World War II has made it possible to carry out regularly contour and temperature analysis of selected pressure surfaces on a hemispheric scale, and hence to prepare upper air maps which may be referred to as normals. It is obviously of great importance to obtain as soon as possible a fairly complete picture of the different meteorological elements. Once a three-dimensional picture of temperature and pressure has been arrived at, the distribution of such derived quantities as temperature lapse-rate, geostrophic wind, geostrophic vorticity, thermal wind and thermal vorticity is easily obtained. More advanced aspects are also visualized; high-speed electronic computers make it possible to compute the three-dimensional fields of the vertical velocity and horizontal divergence associated with the current weather maps, and hence to prepare normal maps for these quantities. If one is justified in extrapolating the present trend in numerical forecasting, it seems likely that detailed upper air information will have to be made available on a routine basis for the purpose of numerical prediction and

[1] Present address: Joint Numerical Prediction Unit, Washington D. C.

[2] Present address: University of Helsinki, Institute of Meteorology, Helsinki.

in a form suitable for the computations of the fields of vertical velocity and horizontal divergence. Although the distribution of these quantities, as expressed by the present atmospheric models used for the purpose of numerical forecasting, may be too crude for the preparation of normals, it is not difficult to design a more refined model for this particular purpose. The efforts needed in order to produce the additional information required by such a model may not be prohibitive from a practical point of view. The availability of current maps for vertical velocities would seem to be an urgent requirement for a complete and successful study of the general circulation.

A question which naturally arises in the discussion of three-dimensional normals, is the form in which these normals should be presented, and in particular whether the usual form is the most suitable one. The present trend would seem to be to give the normal distribution of a certain meteorological element in as many as possible of the 7 pressure levels (1,000, 850, 700 mb etc.) currently reported in routine observations; this, of course, constitutes a fairly complete three-dimensional picture. Still the main characteristics of the vertical distribution may be more easily examined if described by a few properly selected parameters than in the 7-chart presentation. It seems, for instance, likely that the vertical velocity distribution along the vertical could be fairly accurately described in terms of 3 or 4 parameters. A more obvious example is the vertical distribution of temperature with height. The approximate linearity in the normal temperature-height curve suggests immediately the most suitable choice of parameters.

One of the co-authors has shown elsewhere (ÁRNASON, 1952 and 1953) that the main characteristics of the vertical temperature distribution may be described in terms of three parameters, namely, the average temperature lapse-rate in the troposphere, a "representative" sea-level temperature, and the height of the tropopause. A description of this kind gives a clearer picture of the normal distribution of temperature than if displayed by means of the 7 above-mentioned charts.

A treatment of this kind has been applied to height and thickness normals published by the U.S. WEATHER BUREAU (1952) with the aim of studying the main features of the three-dimensional distribution of temperature within the layer 1,000—500 mb. Two months, January and July, were selected, representing a typical winter and summer conditions respectively. The normal temperature-height curve was approximated by a straight line which was adjusted so that the 1,000—700 and 700—500 mb thicknesses were correctly given by the model. Two parameters are needed for the description of the temperature field, the lapse-rate k and the "representative" 1,000-mb temperature τ_0.

Chapter 2 gives the details pertaining to the determination of the two parameters; chapters 3 and 4 are devoted to the discussion of the k- and τ_0-maps, whereas the corresponding thermal wind field is discussed in chapter 5. The main achievement of the investigation laid down in the subsequent chapters is in short as follows:

1. It shows the usefulness of applying a simple model to meteorological normals, presented in the conventional manner, in order to obtain a clear picture of the main characteristics of the vertical distribution.
2. It describes in considerable detail the normal fields of the temperature lapse-rate and the thermal wind, neither of which has been studied earlier to the same extent.
3. It gives a measure of the baroclinity of the lowest layer of the atmosphere which is more representative than the observed temperature of the earth's surface, and which more clearly than the 1,000—700 mb thickness isopleths shows the major frontal zones of the atmosphere.
4. The results strongly suggest that the variation in the thermal wind with height is more pronounced than commonly believed, and that this feature should be given due consideration in the design of models for numerical forecasting.

2. Method of determining the temperature parameters

In the model, referred to in the introduction, the observed normal distribution of temperature with height in the troposphere is replaced by the linear relationship

$$\tau = \tau_0 - kz \qquad (2.1)$$

where τ is the temperature at height z, k the temperature lapse-rate (independent of height), and τ_0 the temperature at $z=0$. The temperature τ_0 may be referred to as a "representative" sea level temperature since it is, as will appear below, much less influenced by the local heat and cold sources at the earth's surface than is the observed one.

One may think of different ways of determining the parameters τ_0 and k. It would seem simplest to determine these from the observed temperatures at different heights, but temperature normals for several levels, having a hemispheric coverage, are not available. On the other hand, the tabulated height normals recently published by the U.S. Weather Bureau can readily be used to determine these parameters. The normals quoted contain 700 and 500 mb heights together with the thickness 1,000—700 mb. We now require that the temperature curve represented by equ. (2.1) gives the same thicknesses of the layers 1,000—700 mb and 700—500 mb as those observed. Moreover, we will for practical purposes have τ_0 refer to the 1,000 mb height rather than sea level; this implies that we from now on refer to the 1,000 mb surface as a zero level. As will now be seen, this requirement makes it possible to determine τ_0 and k uniquely from the thickness normals 1,000—700 mb and 700—500 mb. The general analytical expression for the thickness $z_2—z_1$ of a layer bounded by the two pressure surfaces p_1 and p_2, is

$$z_2 - z_1 = \frac{R}{g}\int_{p_2}^{p_1} T\frac{dp}{p} \qquad (2.2)$$

where T is the observed temperature, R the gas constant for atmospheric air, and g the acceleration of gravity. In order to carry out the integration of (2.2), one needs to know T as a function of p. This is obtained in the model by substituting $-\frac{dT}{k}$ (in virtue of (2.1)) for dz into the hydrostatic equation in the form

$$\frac{dp}{p} = -\frac{g}{R}\frac{dz}{T} \qquad (2.3)$$

and integrating, whereupon the following expression is arrived at:

$$\tau = \tau_1\left(\frac{p}{p_1}\right)^{\frac{Rk}{g}} \qquad (2.4)$$

Carrying out the integration of (2.2) by substituting the expression (2.4) for the temperature we obtain the following expression for $z_2—z_1$

$$z_2 - z_1 = \frac{\tau_1}{k}\left[1 - \left(\frac{p_2}{p_1}\right)^{\frac{Rk}{g}}\right] \qquad (2.5)$$

We now apply (2.5) to the two layers, first of which is bounded by p_0 (= 1000 mb) and p_1 (= 700 mb), and the second one by p_0 and p_2 (= 500 mb). The factor $\frac{\tau_1}{k}$ in (2.5) is then in both cases to be replaced by $\frac{\tau_0}{k}$ and can be eliminated by division. By doing so, we arrive at the following equation for the determination of k:

$$z_1 - z_0 = \frac{1 - \left(\frac{p_1}{p_0}\right)^{\frac{Rk}{g}}}{1 - \left(\frac{p_2}{p_0}\right)^{\frac{Rk}{g}}}(z_2 - z_0) \qquad (2.6)$$

which is easily solved graphically. (The k-lines are straight lines in a $(z_1—z_0)$, $(z_2—z_0)$ diagram). Having determined k, we then find the other parameter τ_0 (= temperature at 1,000 mb) from (2.5), which can either be applied to the layer 1,000—700 mb or the layer 1,000—500 mb. This equation has also a simple graphical solution. The graphs for the

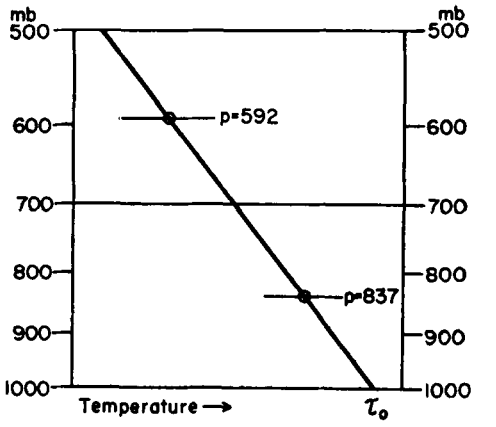

Fig. 1. The temperature-height curve of the model. For explanation see the text.

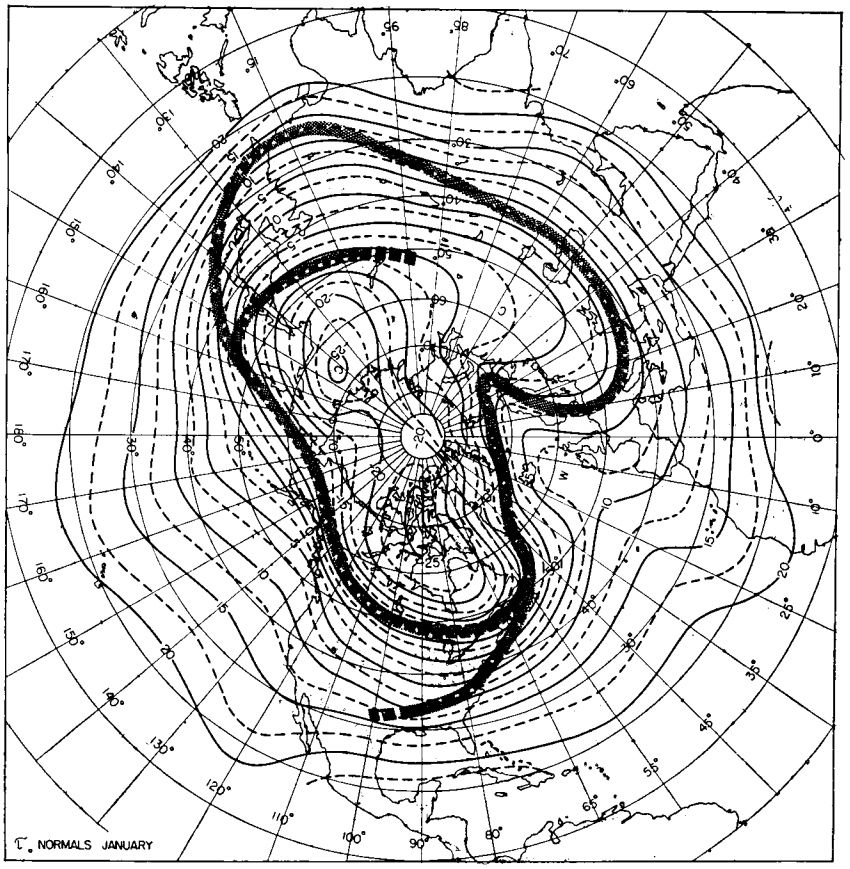

Fig. 2. The distribution of τ_0 for January.

determination of k and τ_0 have not been reproduced here, since their construction is straightforward.

The principle of the method is most easily illustrated if one refers to a p-system (p or a function of p independent variable instead of z). Fig. 1 shows a log p—T diagram where the points corresponding to ½ (log 1,000 + log 700), ½ (log 700 + log 500) and the mean temperatures for the layers 1,000—700 mb and 700—500 mb respectively have been plotted. A straight line through both of these points represents a sounding curve which gives the same thickness for both layers as the observed one. The 1,000 mb temperature, τ_0, is immediately obtained by intersection with the 1,000 mb line and the lapse-rate is determined by the slope. Since in the model we are dealing with z as the independent variable rather than log p, the straight line in the figure is not identical with the height-temperature curve defined above. For the purpose of illustrating the method, however, this difference is unimportant.

3. The τ_0-distribution

Figs. 2 and 3 show the distribution of τ_0 for January and July respectively. It follows from the definition of τ_0 (see fig. 1) that the general pattern of the τ_0-charts can not deviate too much from the pattern of the mean 1,000—700 mb thickness isopleths. Were it not for the non-uniformity in the temperature lapse-rate, the two fields would be identical. Comparison shows that by and large the features are much the same, but it shows also, that in certain regions there are significant differences. Such regions are primarily found along the border lines between the continents and the

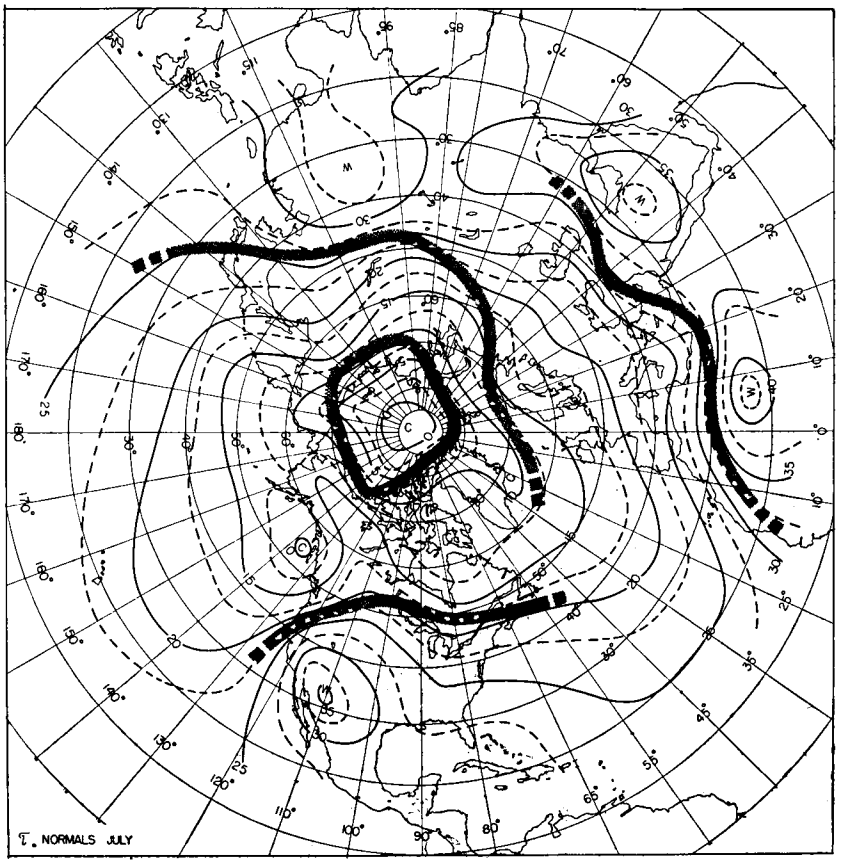

Fig. 3. The distribution of τ_0 for July.

oceans, where particularly strong lapse-rate gradients occur. As appears from the k-charts (see figs. 6 and 7) the cold air is in general more stable than the warm air, and this is particularly the case where the lowest and highest temperatures occur. This is very typical over Siberia and Canada in winter, and over the subtropical parts of the continents in summer. As a result of this, the regions of strongest 1,000—700 mb thickness contrasts will show still more pronounced contrasts on the τ_0-charts, and the concept of a front at sea level is therefore more readily associated with the latter representation of the low-level temperature distribution. In this respect the τ_0-distribution resembles that of the observed sea level and surface temperatures (Handbook of Meteorology, 1945, page 949 and 952), but will on the other hand not show the irregularities of the latter. For this reason we may refer to τ_0 as the "representative" 1,000 mb temperature. It can be shown that an ideal frontal surface would in the τ_0-representation be depicted as a frontal zone just north of the surface front; the width of this zone will depend on the slope of the frontal surface. In the following description of the zones of maximum τ_0-gradients and their relation to the mean positions of the major fronts, this should be born in mind.

The double-hatched zones in figs. 2 and 3 indicate relative maxima in the τ_0-gradients, i.e. zones of maximum low-level baroclinity. One may expect that the positions of these zones are closely related to the positions of the main surface fronts. In his book, "Weather Analysis and Forecasting", figs. 124 and 126, PETTERSSEN presents two hemispheric charts showing the mean position of the principal frontal zones at sea level in winter and

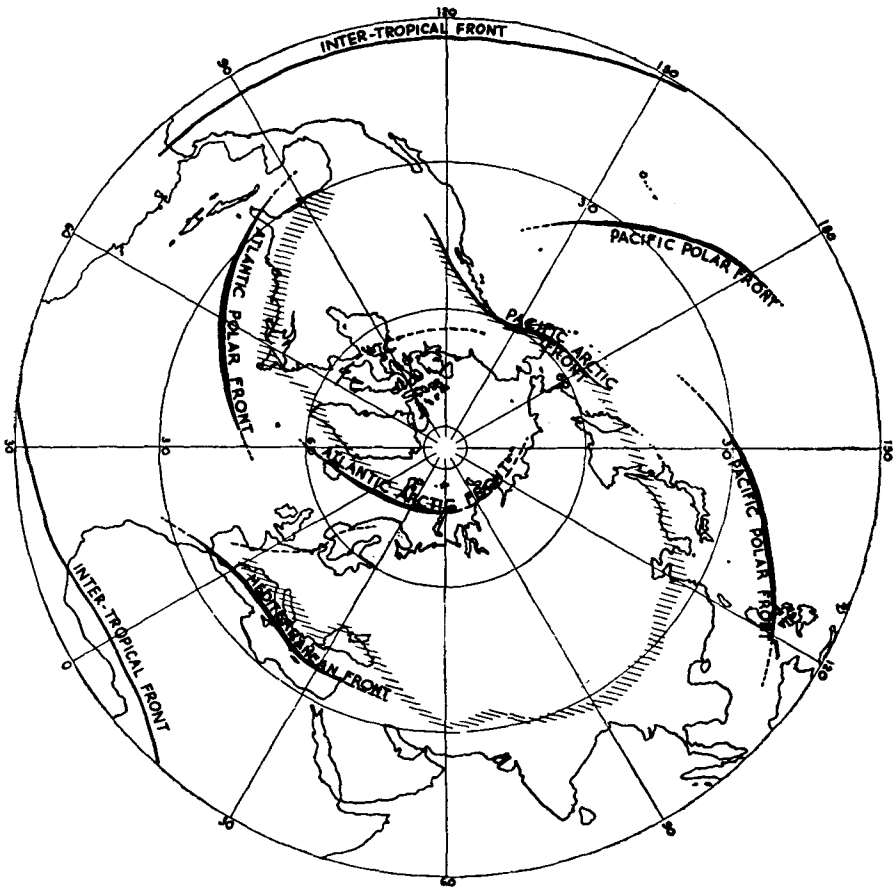

Fig. 4. The principal frontal zones in winter. Hatched zones indicate zones of maximum temperature gradient. (By permission from "Weather Analysis and Forecasting" by S. Petterssen. Copyright May 1954, McGraw-Hill Book Comp., Inc., New York.)

summer, as well as the zones of maximum temperature gradients. These maps have by due permission been reproduced as figs. 4 and 5 in this paper. It is assumed here that the zone of maximum temperature gradients shown in Petterssen's charts refer to low levels, although not specifically stated in his book. Hence, a comparison will be made between the τ_0-distribution for January and July and Petterssen's winter and summer charts respectively, beginning with the winter.

As a whole there is a good agreement between the zones of maximum baroclinity, in particular those connected with the polar and arctic fronts of the Atlantic and Pacific Oceans. The east-west branch of the maximum τ_0-gradient extending from the main zone of the North Pacific and running into Siberia has no corresponding feature in Petterssen's winter chart and is obviously not directly related to any of the principal frontal zones. On the other hand, it is quite clear from the mean sea level pressure distribution for January that the low-level advection favors a concentration of isotherms in this region. As regards the position of the zone of maximum baroclinity over Southern Europe and Asia between the longitudes 15°—80° E, the maximum in the τ_0-gradient is so flat that the hatched zone could have been placed a few degrees of latitude further to the south without violating the data, in which case there would have been a closer agreement between the two charts. The relatively weak maximum in the τ_0-gradient over Western Europe connecting the much stronger maxima

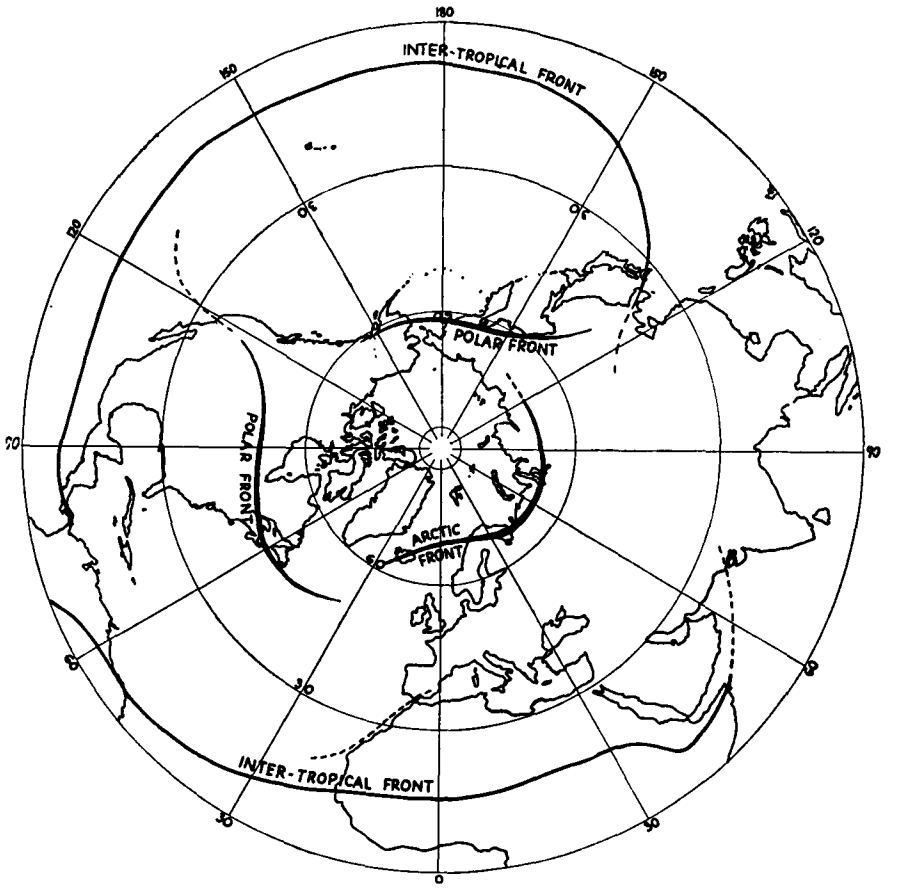

Fig. 5. The principal frontal zones in summer. (By permission from "Weather Analysis and Forecasting" by S. Petterssen. Copyright May 1954, McGraw-Hill Book Comp., Inc., New York.)

over the Arctic Ocean and Southern Europe, is not shown directly by Petterssen, but corresponds to a mean position of a front of secondary importance shown on his map. PALMÉN (1951) has pointed out that over Europe in winter there is often a tendency toward the formation of a surface front between the maritime polar air masses over the western part and the continental polar air over the eastern part of the continent. A glance at the mean sea level pressure chart for January shows that the hatched zone over Central and Southern Europe coincides with the southwestern edge of the continental Eurasian anticyclone.

The particularly pronounced maximum in the τ_0-gradient across the entire North-American continent joining the North-Pacific zone is not shown by Petterssen except for a weak front of secondary importance. The mean sea level distribution over North America shows that the zone of maximum temperature contrasts coincides with the pressure trough between the arctic high and the sub-polar continental one. Palmén has pointed out that the splitting of the continental anticyclone into two parts separated by a secondary front (between the arctic or very cold polar air on one side and the considerably warmer polar air on the other) is a common phenomenon over the United States.

Although we are primarily dealing with low-level phenomena, the τ_0-distribution will in virtue of the thermal wind relationship reflect to a certain extent the wind conditions at high levels. Thus, the two zones of maximum τ_0-gradients over Asia and North America would seem to correspond roughly

to the two main jets found on mean meridional cross sections for the winter months. Reference is made to WILLETT's (1944) well known cross section Swan Island—Bismarck—Barrow during winter showing a subtropical jet between Miami and Nashville (around 28° lat.) and a polar jet over Alaska, and also to MOHRI's (1953) winter cross section along the 140° E meridian which besides the subtropical jet (main jet) also indicates a weak polar jet at latitude 41°.

The τ_0-distribution in July is shown in fig. 3. As one may expect the gradients are much weaker than in winter and their maxima less pronounced. By and large the zones of maximum temperature contrasts coincide with the positions of the principal frontal zones shown by Petterssen (fig. 5). The extension of the Arctic Ocean band of maximum baroclinity across Siberia, China and Southern Japan may not correspond to any major front. On the other hand, such a maximum, although weak, is clearly indicated on the τ_0-distribution, and according to THOMPSON (1951) the West Pacific polar front should be found along the Tibetan Plateau, whereas Petterssen on his summer chart shows no polar front at all over the middle and southern parts of the Asiatic continent.

A feature of particular interest and not shown so clearly in any earlier presentation of the low-level temperature field is the closed excentric zone of maximum baroclinity around the polar cap. In this the northernmost part of the hemisphere we find the largest low-level temperature contrasts. In this connection we refer to SVERDRUP's (1953) experience about the atmospheric disturbances over northeastern Siberia and the Polar Sea during the "Maud"-expedition 1918—1925. According to him, the anticyclonic type of weather predominated in this area during October—April. In May a transition to summerlike conditions appeared as the weather became of more cyclonic character. "In summer several disturbances apparently were formed along a quasistationary front, which was running approximately east-west and was colder on the northern side." In September a transition to winter conditions appeared. It is likely that the circumpolar zone of maximum τ_0-gradient on the July map corresponds to the frontal zone mentioned by Sverdrup.

In much lower latitudes there is another well marked zone of maximum temperature gradient extending from the coast of West Africa to the interior of Asia north of the Gulf of Persia. Its position is just north of the main desert regions and the crowding of the τ_0-lines simply reflects the enormous heating of the Sahara desert as well as the deserts of western Asia. The westernmost part of this zone corresponds roughly to the boundary between the northeast trades and the West-african monsoon and is indicated on Petterssen's summer map as a front of secondary importance. One might expect some cyclone activity along the above mentioned zone, but according to BIEL (1944) fronts and cyclones are rare in the Mediterranean during the summer. The overall lack of rain and cloudiness in this region is of course closely related to the dryness of the air masses involved.

Zonal mean values for τ_0 are shown in fig. 10 as a function of latitude.

4. The *k*-distribution

Figs. 6 and 7 show the *k*-isopleths for January and July respectively drawn at intervals of 0.5° C km^{-1}. The letters S and I indicate respectively minima and maxima in the temperature lapse-rate. To the authors' knowledge, maps showing the normal distribution of temperature lapse-rate on a hemispheric scale have not been published earlier, and it is therefore felt that a discussion of the *k*-maps in some detail may be appropriate. The main features of these maps may, however, first be summarized as follows:

1. The pattern is more broken up than on the corresponding maps for τ_0.
2. In January the lapse-rate is in general low over the continents and high over the oceans at middle and high latitudes. These conditions are reversed in July.
3. Regions of lowest lapse-rates are northern Canada and northeastern Siberia in January and lat. 80°—90° in July. The highest values are found just south of Iceland and over the northernmost part of the Pacific in January and over the desert areas of the subtropical continents in July.
4. The strongest gradients occur along the coasts of the continents north of latitude 50° in January and north of latitude 70° in July.

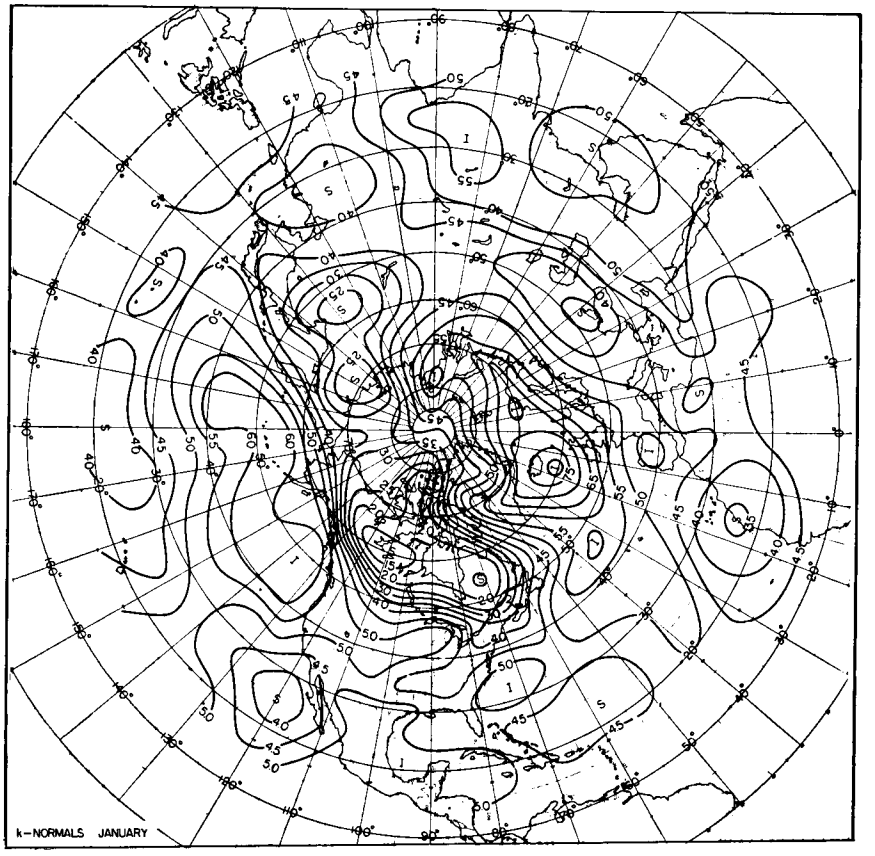

Fig. 6. The distribution of k for January. An S indicates a relative minimum and an I a relative maximum in the temperature lapse-rate.

5. There is a belt of low temperature lapse-rate around 5° of latitude south of the subtropical high pressure girdle at sea level.

The facts listed above are qualitatively well known from physical considerations and synoptic experience, although not demonstrated quantitatively to the same extent earlier. The main features of the geographical-seasonal distribution of temperature lapse-rate is, of course, essentially explained by the geographical location of heat and cold sources and their seasonal shifting. A part of the explanation is also the overall subsidence in the cold continental air and the compensating convergence over the oceans in winter, and the convergence over the continents and the divergence over the oceans in summer.

Although recognized qualitatively, the quantitative measure of some of the main features of the k-distribution may seem surprising. This is to some extent the case of the extremely strong gradients in winter between Iceland and Canada as well as the zone of strong gradients running across the North American continent through Alaska and into the North Pacific. As shown in the last section, these strong k-gradients cause substantial change with height in the thermal wind. More remarkable is perhaps the very strong k-field over the Arctic in July. The magnitude of the k-gradients in this region is comparable with the strongest gradients occurring during January. The occurrence of considerable contrasts in temperature lapse-rate between the ice-covered polar cap and the extensively heated continental surroundings in summer is a priori plausible, since the temperature of the ice can not exceed 0° C, but the strength of this field is in general not realized. It must,

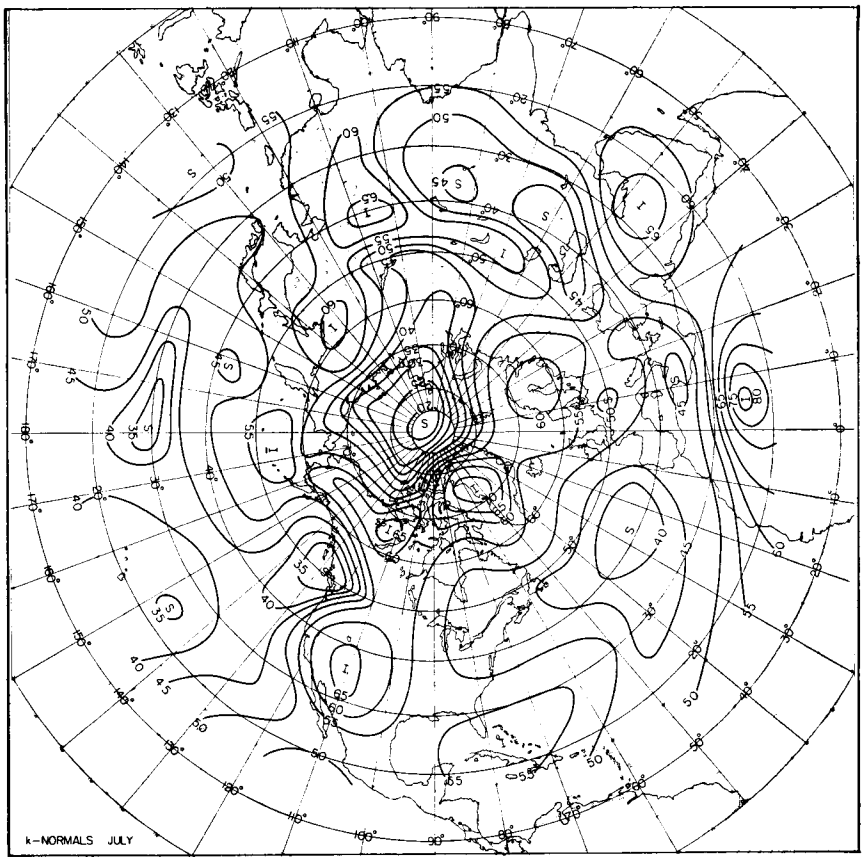

Fig. 7. The distribution of k for July. An S indicates a relative minimum and an I a relative maximum in the temperature lapse-rate.

of course, be born in mind that the analysis over the high Arctic is not as reliable as further south, and for this reason too much emphasis cannot be put upon the details. On the other hand, it is known that the height and thickness normals, upon which the k-charts are based, were carefully tested with regard to consistency of the temperature field; it therefore seems reasonable to have considerable faith in the main features of the k-distribution even at these high latitudes. A few spot checks have been possibly by comparing mean winter and summer soundings compiled by FLOHN (1950) for the arctic stations Tromsö (69°5 N, 19° E), Spitzbergen (78° N, 13°5 E, summer only), Point Barrow (71° N, 156° W), Franz Josef's Land (80° N, 53° E, winter only) and Jakutsk (62° N, 129° E, winter only). These soundings were in good agreement with the k-charts, as far as could be judged by comparing lapse-rate values for two extreme months with seasonal averages. As to the details in January map, the following is pointed out:

a. The trough of low lapse-rate extending from the interior of Canada to the southern part of the United States may correspond to the southern edge of the sinking polar air, whereas the relatively high lapse-rate between Bermuda and the coast of U.S. may reflect the heating of the cold continental air when flowing out over the warm water of the Gulf Stream. The synoptic conditions are similar over the easternmost part and the coastal water of the Asiatic continent, and the details of the k-charts are much alike in these two regions.

b. The area of large lapse-rates over the northern part of the Atlantic with Iceland as a center, is essentially explained by the frequent outbreaks of cold continental air from Canada

and the Greenland area. These outbreaks have long overwater trajectories before reaching the middle and eastern part of the Atlantic and may therefore be expected to have become fairly unstable. More direct outbreaks between Norway and Greenland are not uncommon and in spite of the shorter trajectory the relatively warm water over which the air flows will cause a considerable increase in the lapse-rate. The relation between decrease in stability and the distance travelled by cold air from the North American continent has been investigated by BERSON and PETTERSSEN (1943). They found that atmospherics might occur in the air mass at a distance exceeding 1,000 st. miles from the coast. They also showed a rapid decrease in the frequency of atmospherics south of about 45° N.

As to the details of the July map the following is mentioned:

a. There is a pronounced maximum in the lapse-rate around 65° N, i.e. approximately 5° of latitude north of the low-pressure belt (see fig. 10b) at sea level. The high lapse-rate is apparently closely connected with the frequent cyclonic activity in these latitudes during summer.

b. The western parts of the oceans show larger lapse-rates than the eastern. This agrees well with the synoptic fact that the tropical maritime air is less stable in the western halves of the anticyclonic cells than in the eastern halves.

So far it has not been mentioned that the Normal Weather Charts (1952) give observed 700 mb temperatures tabulated in the same way as the height and thickness values utilized here. In reference to fig. 1, this implies that one additional point of the temperature height curve is known besides those marked in the figure. Obviously this extra piece of information provides an additional knowledge of the stability conditions of the 1,000—500 mb layer and makes it to a certain extent possible to distinguish between the two sub-layers 1,000—700 mb, and 700—500 mb. In order to do so, the observed 700 mb temperatures have been subtracted from the corresponding 700 mb temperatures computed by means of equ. (2.1), using the appropriate τ_0- and k-values. In general the differences will not be zero, and they are obviously a rough measure of the deviation in the lapse-rates of the two sub-layers from the k-values. A negative value of a difference means in general that the lapse-rate of the layer 1,000—700 mb is less than the lapse-rate given by the k-value, whereas the layer 700—500 mb has a lapse-rate exceeding the k-value, i.e. the lowest layer is the more stable one. A positive value on the other hand indicates that the uppermost layer is the more stable one. In converting the differences of the two sets of 700 mb temperatures into differences in lapse-rate, we may for practical purposes assume the thicknesses of both layers to be the same and equal to 2.5 km. This means that a difference of 1° C corresponds to a deviation of 0.4° C km^{-1} in the lapse-rate of each layer from the appropriate k-value, i.e. the lapse-rates of the 1,000—700 mb and 700—500 mb layers differ 0.8° C km^{-1}.

A study of these 700 mb temperature differences gave the following results:

1. On the average the lapse-rate of the layer 1,000—700 mb is slightly less than the lapse-rate of the layer 700—500 mb. This difference is very small in July, whereas it in January is well marked in the latitudes 40°—70° having a maximum of 1.6° C km^{-1} at 60° (each of the layers deviates 0.8°C km^{-1} from the k-value). South of latitude 30° and north of latitude 80° the conditions seem to be reversed both in July and January, i.e. the uppermost layer is the more stable one. The difference is less than 0.4 in the low latitudes but varies from 0.4—1.0 in the high latitude belt. Here, of course, one must bear in mind the uncertainty of data near the north pole as well as in the low latitudes.

2. There is a pronounced seasonal variation over the continents at middle and high latitudes. In January the layer 1,000—700 mb is by far the more stable one, this is particularly the case between the cores of the Canadian high and the Icelandic low and also over northeastern Siberia between the continental high and the Aleutian low. The maximum lapse-rate difference between the two layers is 3.2° C km^{-1}, but does in most places not exceed 1.6°C km^{-1} in the regions mentioned. In July the conditions tend to be the opposite over the continent, but in general the difference in lapse-rate between the two layers is considerably less than in January. Maximum values of 2.4°C km^{-1} occur over the interior

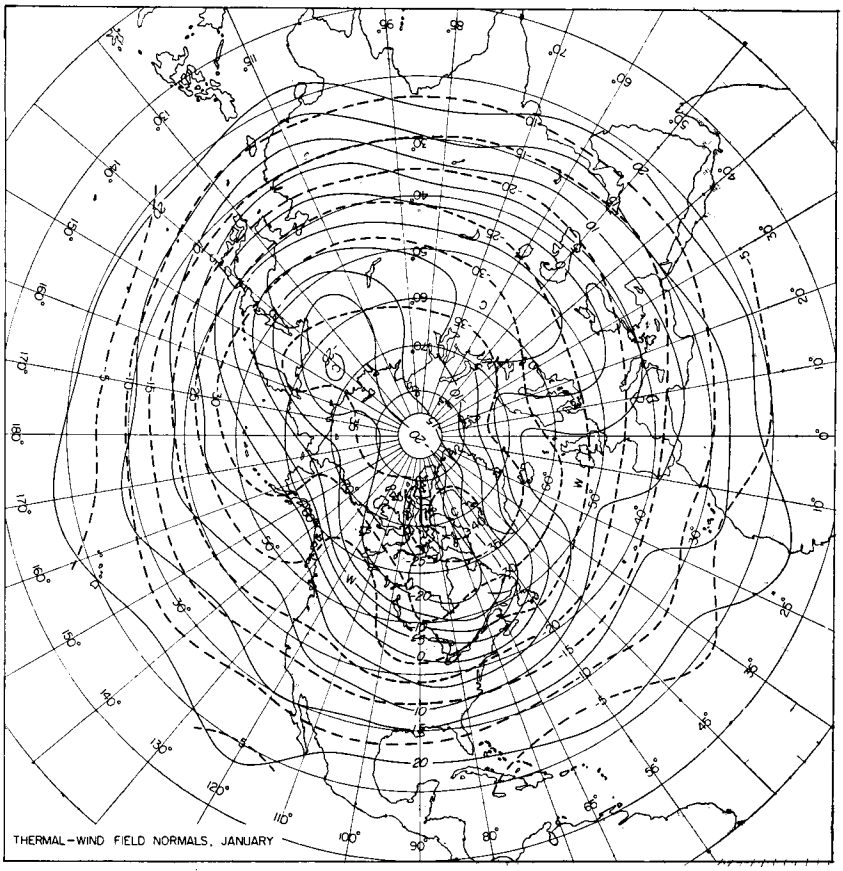

Fig. 8. The thermal wind distribution at 1,000 mb (solid lines) and 500 mb (broken lines) for January. For further explanation see the text.

of Asia north of lat. 45° and over the northwesternmost part of the U.S.A.

3. In addition to the overall picture given above, there are some details deserving of mention. Such details are the two comparatively small areas of positive differences in the 700 mb temperatures (1,000—700 mb layer the less stable one) in January off the east coast of Japan and over the Atlantic south of Greenland and east of Newfoundland. The first of these two is the more pronounced. One is inclined to explain the existence of these two regions as a result of the rapid heating of the cold continental air when it travels over the much warmer ocean as discussed earlier. Another feature of interest in January is an oblong area at around lat. 75°N running from the east coast of Greenland to longitude 75°E where the layer 1,000—700 mb is considerably less stable than the layer 700—500 mb. Apparently these large low-level lapse-rates in this region are to some extent a result of the considerable cyclone activity there, but may also reflect a certain lack of thermal consistency in the analysis of the normal height maps. Noteworthy features in July are that whereas the Azores high hardly shows any preference for higher stability in the lower layer, the Pacific high is very much more stable below 700 mb than above. It is finally mentioned that north of lat. 80° there are indications that the layer 700—500 mb is the more stable one during July.

Zonal mean values for k are shown in fig. 10 as a function of latitude.

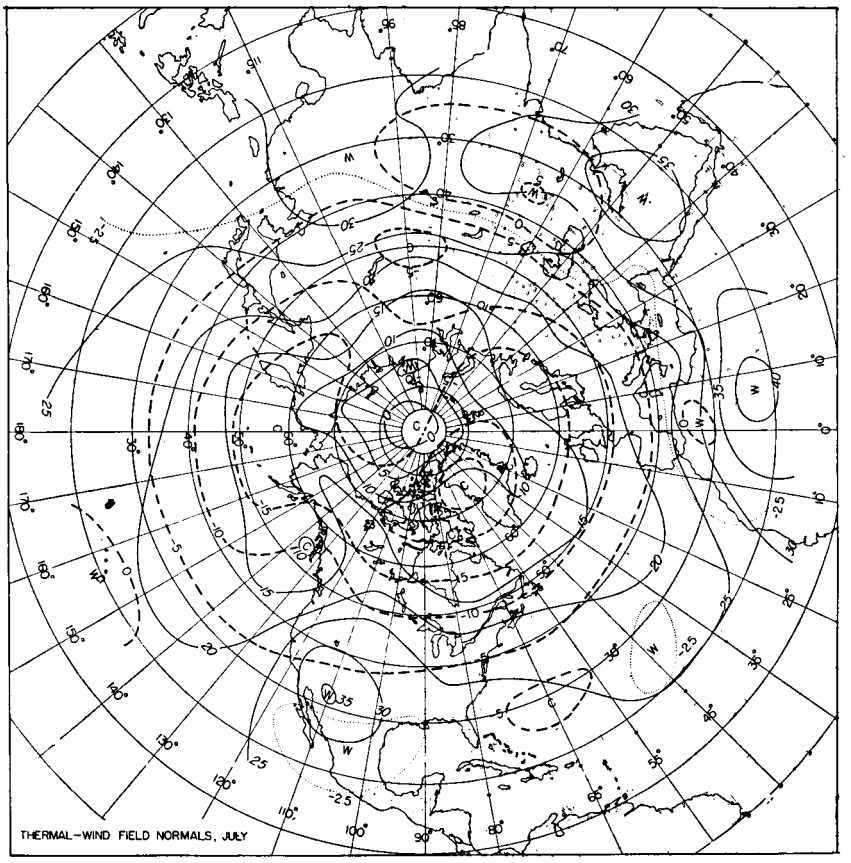

Fig. 9. The thermal wind distribution at 1,000 mb (solid lines) and 500 mb (broken lines) for July. For further explanation see the text.

5. The thermal-wind field

If $\mathbf{v}$ denotes the geostrophic wind, $\frac{\partial \mathbf{v}}{\partial z}$ is the thermal wind, commonly expressed in terms of the horizontal temperature ascendent as follows:

$$\frac{\partial \mathbf{v}}{\partial z} = \frac{g}{fT}\mathbf{k} \times \nabla T \qquad (5.1)$$

where $\mathbf{k}$ is a unit vector directed vertically upward and f is the Coriolis parameter. We now substitute in equ. (5.1) the temperature of the model, as given by equ. (2.1), and obtain the following expression for the thermal wind

$$\frac{\partial \mathbf{v}}{\partial z} = \frac{g}{f\tau}\mathbf{k} \times \nabla \tau = \mathbf{v}' - z\mathbf{v}'' \qquad (5.2)$$

where

$$\mathbf{v}' = \frac{g}{f\tau}\mathbf{k} \times \nabla \tau_0; \quad \mathbf{v}'' = \frac{g}{f\tau}\mathbf{k} \times \nabla k \qquad (5.3)$$

The variation with height in $\frac{1}{\tau}$ is unimportant, and we may therefore for practical purposes consider the vectors $\mathbf{v}'$ and $\mathbf{v}''$ as independent of z. Consequently, the thermal wind varies linearly with height. Since there is strong empirical evidence for the linearity with height in the temperature, in particular when averaged in time, we believe that equ. (5.2) gives an essentially correct picture of the normal distribution of the thermal wind. It is pointed out that in spite of the simple thermal distribution, the model allows not only for a

change in magnitude, but also for a change in direction of the thermal wind with height.

It appears from equ. (5.3) that the vectors $\mathbf{v}'$ and $\mathbf{v}''$ are related to the parameters τ_0 and k in a similar way as the geostrophic wind is related to the contour lines; obviously $\mathbf{v}'$ is the thermal wind at $z=0$ (= 1,000 mb), whereas $\mathbf{v}''$ expresses the constant rate of change with height. It now follows that the τ_0-and k-maps together depict the field of thermal wind. Since the isotherms are drawn for every fifth degree centigrade, and the lapse-rate isopleths for an interval of $5 \cdot 10^{-4}$ °C m^{-1}, the two right hand terms in equ. (5.2) are equal in magnitude at $z = 5$ km wherever the k-lines are twice as dense as the τ_0-lines. Having this in mind, an inspection of the two maps immediately reveals that in certain regions there is a very considerable variation in the thermal wind with height, particularly in winter.

In order to show this variation more clearly, the temperature τ_5 at the 500 mb level has been computed by means of equ. (2.1) and its isopleths at 5°C interval superimposed upon the τ_0-maps; those are shown in figs. 8 and 9. The solid lines are the τ_0-isopleths and the dashed lines the isotherms of the 500 mb surface. An equal spacing of the two sets of curves corresponds to the same magnitude of the thermal wind, and its direction is along the respective isotherms with the lowest temperature to the left. Although these two maps primarily show the isobaric distribution of temperature, it is convenient to refer to them as thermal wind maps in virtue of the relationship expressed by the equations (5.2) and (5.3). By the aid of the thermal wind charts, one can easily study the change with height of the thermal wind.

The main features of the thermal wind distribution with increasing height may be summarized as follows:

1. Pronounced change both in magnitude and direction at middle and high latitudes.
2. General tendency toward more regular pattern and toward predominance of zonal direction.
3. Strong variation in regions of pronounced low-level temperature advection. Typical regions of this kind in winter are the Newfoundland—Greenland—Iceland area and Western Europe.

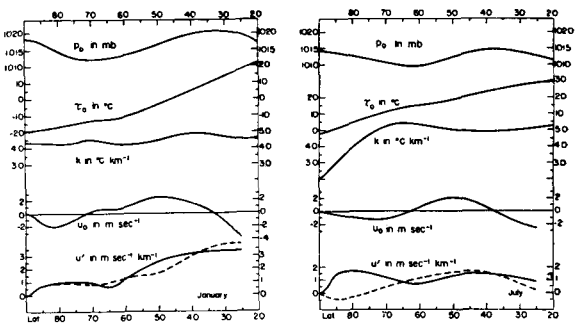

Fig. 10. Zonal means for the sea level pressure p_0 and the corresponding geostrophic wind u_0, the parameters τ_0 and k as well as the thermal wind u' at 1,000 mb (solid lines) and 500 mb (broken lines), a) for January, b) for July.

4. Extremely great decrease in magnitude in January over the northeasternmost part of Siberia, Alaska and western and southern Canada.
5. Marked decrease over the Arctic in July.

The zonal mean of the thermal wind, denoted by u' is shown in fig. 10 as a function of latitude. The solid curves refer to the 1,000 mb and the dashed ones to the 500 mb level. For the computation of u', central differences in the zonal means of the respective temperatures comprising ten degrees of latitude were used. One notices the minima in the thermal wind at 1,000 mb at lat. 65° and 60° in January and July respectively, which reflect the overall weak low-level temperature gradient in these latitudes. Noteworthy is the strong thermal wind at 1,000 mb in high latitudes in July and its rapid decrease with height, resulting in the reverse direction at 500 mb north of latitude 75°. There are presumably some doubts as to the reality of this reversal. In the first place, the upper air analysis north of latitude 60° but south of 75° is based upon a sparse network of stations and in the second, the analysis north of latitude 75° is practically a mere extrapolation of the contour distribution to the south.

Acknowledgement

The authors wish to express their thanks to the technical staff of the Institute of Meteorology, University of Stockholm; in particular to Miss B. WICKBERG who drafted the figures and Mrs. U. TABATABAI who carried out most of the computations for the preparation of the charts.

REFERENCES

ÁRNASON, G., 1952: A baroclinic model of the atmosphere applicable to the problem of numerical forecasting in three dimensions. I. *Tellus*, 4, 356—373.

—, 1953: A baroclinic etc. II. *Ibid.*, 5, 386—402.

BERRY, F. A., et al., 1945: *Handbook of Meteorology*, New York, McGraw-Hill Comp., pp. 949 and 952.

BERSON, F. A., and PETTERSSEN, S., 1943: Atmospherics in relation to fronts and air masses. A report of *Meteorological Research Committee, Air Ministry*, London, 7 pp.

BIEL, E. R., 1944: Climatology of the Mediterranean area. Univ. of Chicago, Dep. of Meteorology, *Miscellaneous Reports* No. 13, pp. 12 and 135.

FLOHN, H., 1950: Grundzüge der allgemeinen atmosphärischen Zirkulation auf der Südhalbkugel. *Arch. Met. Geophys. und Bioklimat., A*, 2, 17—64.

MOHRI, K., 1953: On the fields of wind and temperature over Japan and adjacent waters during winter of 1950—1951. *Tellus*, 5, 340—358.

PALMÉN, E., 1951: The aerology of extratropical disturbances. *Compendium of Meteorology*, Amer. Met. Soc., Boston, Mass., pp. 599—620.

PETTERSSEN, S., 1940: *Weather Analysis and Forecasting*. New York, McGraw-Hill Comp., pp. 269 and 271.

SVERDRUP, H. U., 1953: *North Polar Expedition with the "Maud", 1918—1925*. Vol. 2, Part 1. Bergen, A. S. J. Griegs Boktrykkeri, pp. 324—325 and 328.

THOMPSON, B. W., 1951: An essay on the general circulation of the atmosphere over South-East Asia and the West Pacific. *Quart. J. R. Met. Soc.*, 77, 569—597.

U.S. Dep. of Commerce, Weather Bureau, 1952: *Normal Weather Charts for the Northern Hemisphere*. Technical Paper No. 21. Washington, D. C., Government Printing Office, 74 pp.

WILLETT, H. C., 1944: *Descriptive Meteorology*. New York, Academic Press, Inc., p. 132.